Predictions in Ungauged Basins: PUB Kick-off (Proceedings of the PUB Kick-off meeting held in Brasilia, 20–22 November 2002). IAHS Publ. 309, 2007.

Differences in area-averaged rainfall depth over a mid-size basin from two remote sensing methods of estimating precipitation

DANIEL F. BARRERA[1], EDUARDO B. CEIRANO[2] & GRACIELA V. ZUCARELLI[2]

1 *Departamento de Ciencias de la Atmósfera y los Océanos–FCEN, Universidad de Buenos Aires / CONICET, Ciudad Universitaria, 1428 Buenos Aires, Argentina*
barrera@at.fcen.uba.ar

2 *Facultad de Ingeniería y Ciencias Hídricas- Universidad Nacional del Litoral*

Abstract Accumulated rainfall fields over the Feliciano River basin (5500 km^2 in a subtropical humid region in eastern Argentina) were obtained for 3-h and 6-h consecutive periods during three days in which intense storm activity took place. Three different rainfall fields were obtained for each of the abovementioned periods, corresponding to three ways of estimating precipitation from GOES IR images: The first one, by applying the "autoestimator" technique by Vicente *et al.* (1998); the second and third ones, by applying a modification to this technique consisting of generating synthetic bright temperature images every 10 min by interpolation in time and space from two consecutive GOES IR images. This modification allows the displacement of cloud systems (driven by the dominant winds) to be taken into account over the region between two consecutive satellite images. In the second method of rainfall estimation, movement of cloud systems was assumed to be driven by the displacement of mid-tropospheric layers, while in the third method upper-tropospheric layers were used (with cloud tops brightness temperature from 268ºK to 253ºK in the first case, and from 248ºK to 233ºK in the second case). Area-averaged rainfall amounts over the sub-basins were obtained by computing the arithmetic mean of the pixel values over all the pixel centres inside each sub-basin. To accomplish this task, the basin map and its divisions, which were digitized on a Transverse Mercator Projection, were transformed to geographical coordinates, as was done with the satellite images from Oblique Stereographic Projection. While the latter two methods of precipitation estimation (both using observed and synthetic bright temperature images) gave little differences on area-averaged rainfall over the 17 sub-basins of the watershed, the first one gave significant differences compared to the latter ones in both total amount and spatial distribution, especially in the location of centres of maximum values. These differences were found in most of the periods considered for both the 6-h and the 3-h consecutive period sets, and were especially strong for intense precipitation periods (up to 40% increase in some sub-basins when using synthetic images). When changing from 6-h to 3-h consecutive periods, the comparison between area-averaged rainfall values obtained with the first and the two other methods of estimation (with and without time-interpolated synthetic temperature images) showed a significant increase in the differences in time distribution of rainfall depths. The results show that the modification introduced in the "autoestimator" technique allows the capture of the displacement of raining cloud cells, which at the same time causes significant differences in estimated rainfall amounts over areas smaller than the size of the studied watershed.

Key words areal rainfall; precipitation estimates; remote sensing; watershed

INTRODUCTION

The accuracy of areal rainfall estimates obtained from a raingauge network was investigated and discussed by several authors, who showed that because of rainfall variability these estimates are strongly affected by errors in most cases (see for example Horton, 1923; Lebel *et al.*, 1987).

In this paper we discuss the differences in point precipitation and area-averaged rainfall depth over a mid-size basin when a method to generate synthetic bright temperature images is introduced into a more general technique to estimate rainfall fields from GOES data. This technique, known as "auto-estimator" (AE) was proposed by Vicente *et al.* (1998) and was applied in the study area in a former paper (Barrera *et al.*, 2002).

The studied area was the Feliciano River basin (5500 km^2) located in a subtropical humid region in the eastern part of Argentina.

METHODOLOGY AND APPLICATION

Accumulated rainfall fields over the Feliciano River basin were obtained for 3-h and 6-h consecutive periods during three days in which intense storm activity took place.

Area-averaged rainfall amounts over the 17 sub-basins of the watershed were obtained by computing the arithmetic mean of the pixel values over all the pixel centres inside each sub-basin. To accomplish this task, the basin map and its divisions, which were digitized on a Transverse Mercator Projection (Fig. 1), were transformed to geographical coordinates and integrated to a regional map (Fig. 2). Also, pixels locations were posted over the studied basin (Fig. 3).

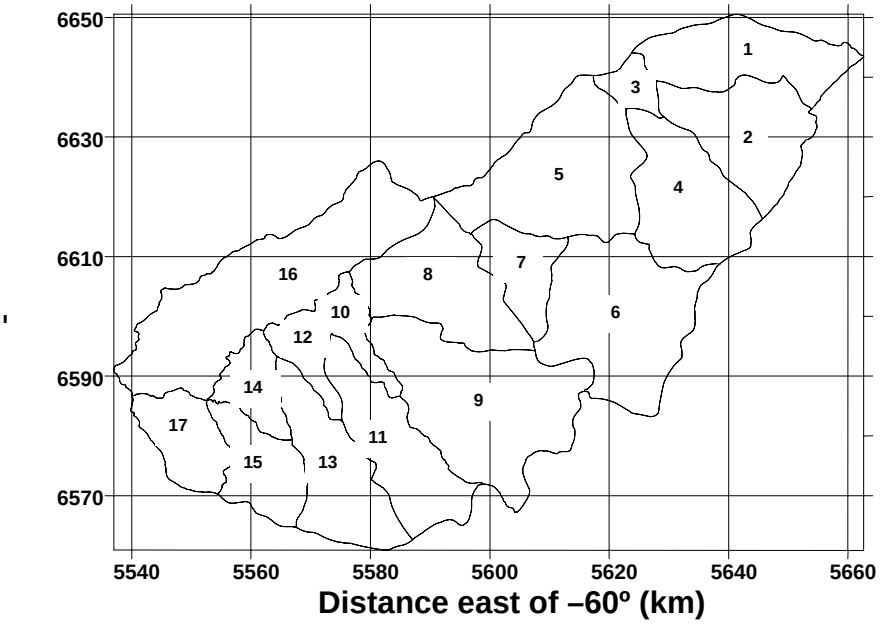

Fig. 1 Sub-basins of the Feliciano River basin. Gauss-Krüger Projection.

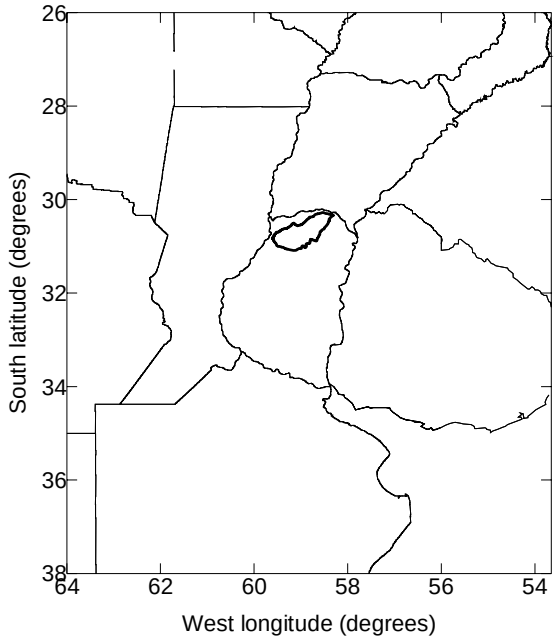

Fig. 2 Location of the Feliciano River basin in the Province of Entre Rios (Argentina).

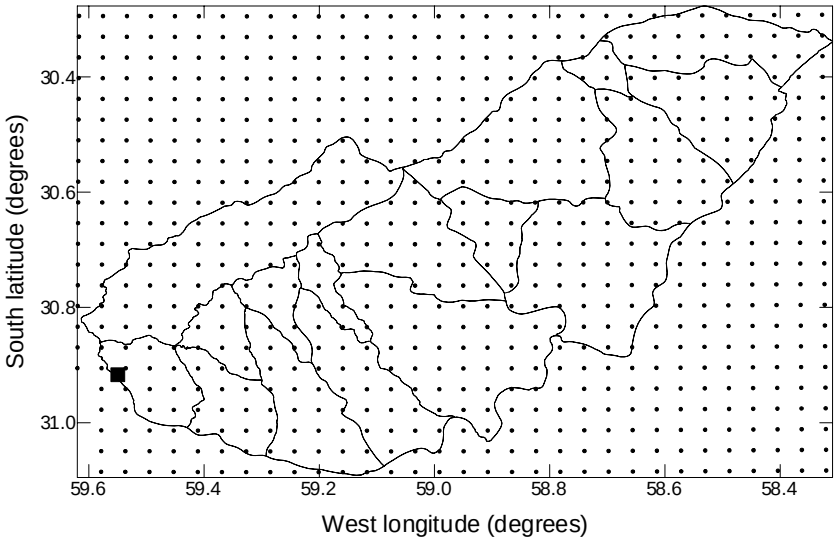

Fig. 3 Location of pixel centres and Paso Medina over the watershed.

Three different rainfall fields were obtained for each of the abovementioned periods, corresponding to three different procedures of estimating precipitation from GOES IR images, all of them applying the AE technique: The first one, by using only the observed GOES IR images (referred as procedure 1); the second and third ones (referred to as procedures 2 and 3), by using observed and synthetic images; these synthetic bright temperature images were generated every 10 mins by interpolation in time and space from two consecutive GOES IR images. This modification allows cloud systems displacement to be taken into account (driven by the dominant winds) over the region between two consecutive satellite images. In procedure 2, movement of

cloud systems was assumed to be driven by the displacement of mid-tropospheric layers, while in procedure 3 upper-tropospheric layers were used (with cloud tops brightness temperature from 268ºK to 253ºK in the first case, and from 248ºK to 233ºK in the second case).

RESULTS

While the latter two ways of precipitation estimation (both using observed and synthetic bright temperature images and referred to as procedures 2 and 3) gave small differences on area-averaged rainfall over the 17 sub-basins of the watershed, procedure 1 gave significant differences compared to the latter ones in both total amount and spatial distribution, especially in the location of centres of maximum values (Figs 4 and 5).

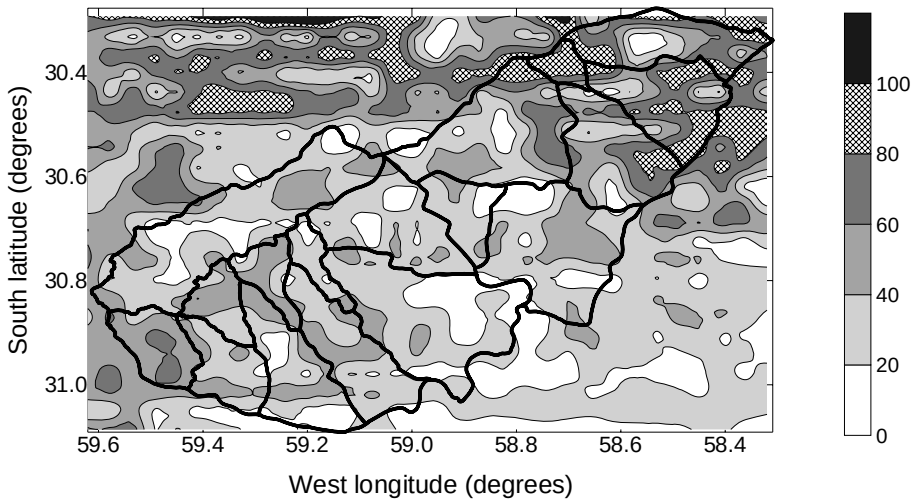

Fig. 4 Estimated rainfall. Technique AE with observed images only.

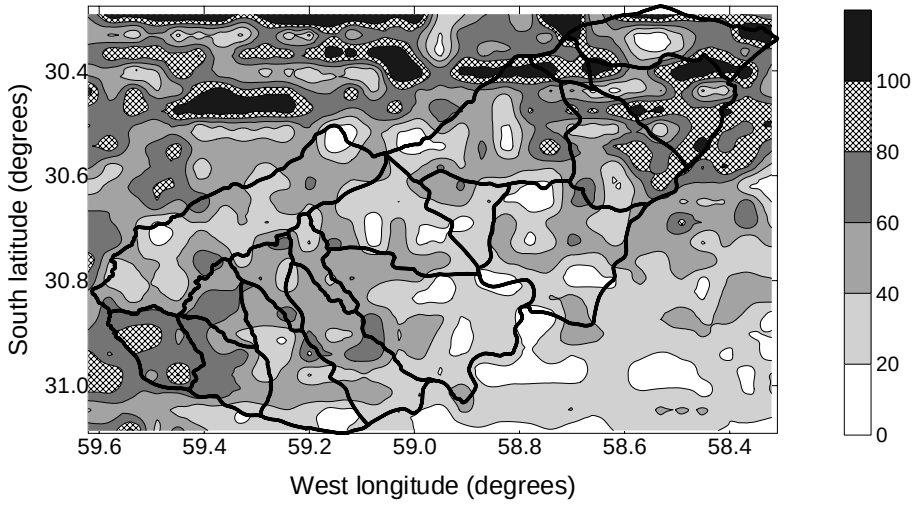

Fig. 5 Estimated rainfall. Technique AE with observed and synthetic images.

These differences were found in most of the periods considered for both the 6-h and the 3-h period sets, and were especially strong for intense precipitation periods (up to 40% increase in some sub-basins when using synthetic images, as shown in Figs 6 and 7).

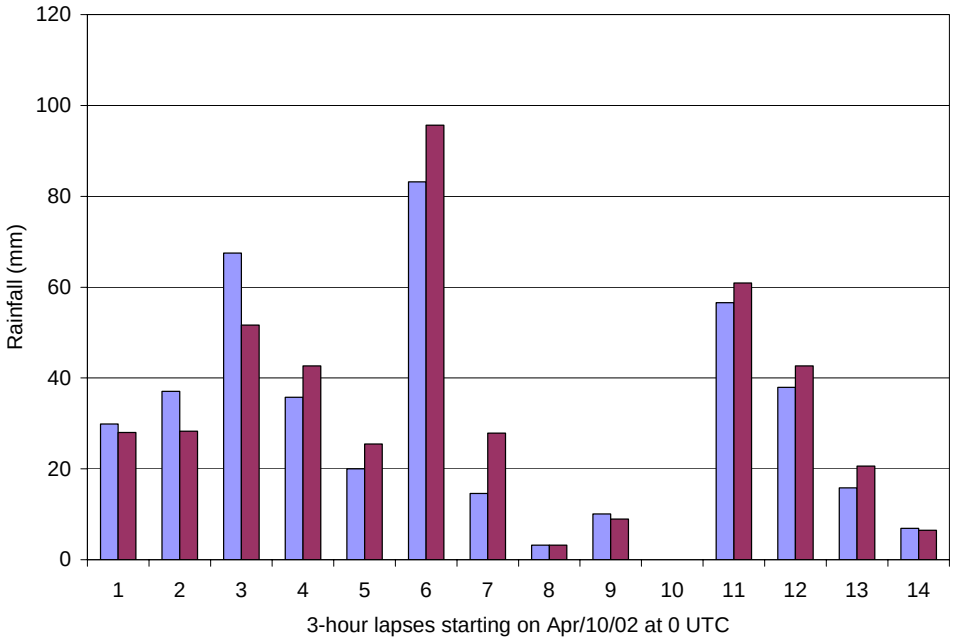

Fig. 6 Estimated rainfall over sub-basin 1. Left bars: Procedure 1. Right bars: Procedure 2.

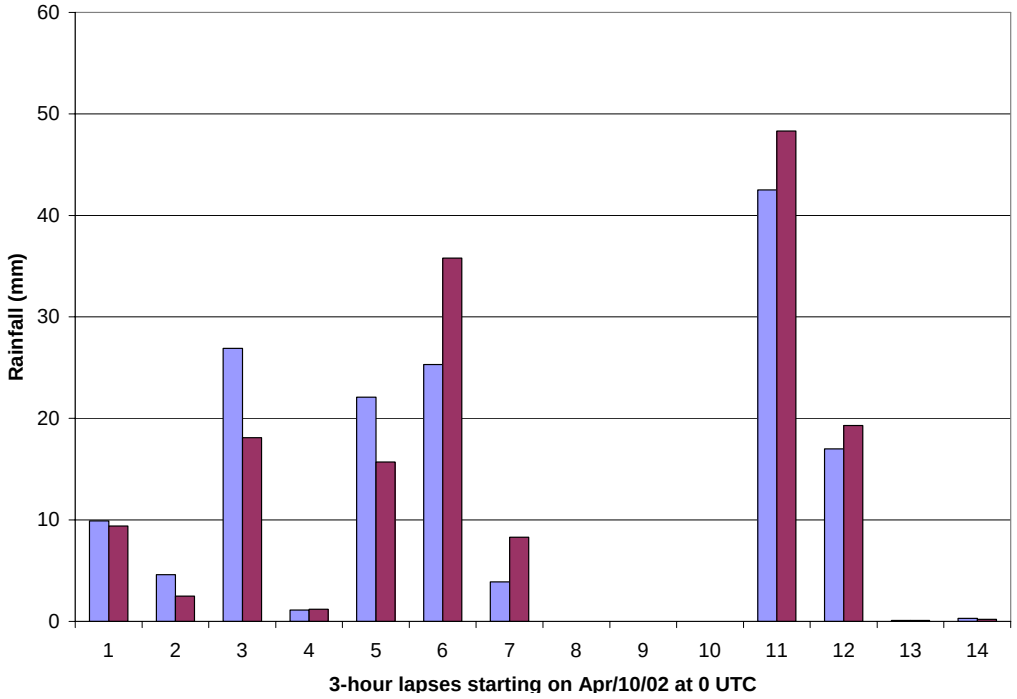

Fig. 7 Estimated rainfall over sub-basin 13. Left bars: Procedure 1. Right bars: Procedure 2.

Accumulated precipitation every 6 h were obtained from 12UTC (09:00 h local time) to 12UTC of the following day, during 9–12 April 2002 following procedures 1 and 2.

Tables 1 and 2 give the distribution of area-average rainfall in 6-h lapses for the rainy period beginning the 10 April at 0UTC and the 17 sub-basins, obtained from procedures 1 and 2, respectively.

Table 1 Distribution of area-average rainfall over the sub-basins. Procedure 1.

Sub	1	2	3	4	5	6	7	8	9	10	11	12	13	14	15	16	17
Pixels	22	21	4	24	36	35	11	25	39	6	20	9	21	8	13	46	12
00–06	0	0	0	0	0.5	0	0.1	0.7	0	0.2	0.1	0	0.3	0.2	0.9	0.1	0.6
06–12	67.0	60.3	84.5	59.4	46.7	37.1	39.1	30.3	26.3	27.6	17.5	27.6	14.5	14.1	18.8	27.2	16.6
12–18	103.3	123.4	157.8	119.7	115.8	102.5	105.0	70.8	62.6	72.0	42.4	60.3	28.0	40.3	23.8	49.3	21.2
18–24	103.2	104.1	120.9	82.1	72.5	48.2	48.0	50.3	49.8	54.9	67.7	74.8	47.4	81.8	78.7	55.1	102.1
24–30	17.8	13.4	18.6	12.6	15.3	8.2	12.4	9.5	8.8	2.9	7.7	10.4	3.9	9.4	8.4	5.2	11.0
30–36	66.7	54.1	67.6	49.8	41.4	52.7	38.2	22.2	30.1	26.5	49.9	47.8	42.5	46.8	59.2	32.4	49.2
36–42	53.8	48.8	50.5	28.6	23.3	20.2	18.2	18.2	23.5	20.5	18.6	23.3	17.1	18.0	13.1	15.5	3.9
42–48	7.0	4.1	3.2	3.7	3.0	2.5	2.4	0.9	0.4	0.3	0.2	0.3	0.3	0.3	0.1	0.7	0.2
48–54	0.1	0.1	0.1	0.1	0.1	0	0.1	0	0	0	0	0	0	0	0	0	0

Table 2 Distribution of area-average rainfall over the sub-basins. Procedure 2.

Sub	1	2	3	4	5	6	7	8	9	10	11	12	13	14	15	16	17
Pixels	22	21	4	24	36	35	11	25	39	6	20	9	21	8	13	46	12
00–06	0	0	0	0	0.4	0	0.1	0.5	0	0.2	0.1	0	0.3	0.2	0.7	1.1	0.4
06–12	56.3	52.6	70.2	48.1	45.0	28.6	33.6	27.5	17.9	21.8	12.9	16.3	11.9	10.6	15.1	24.0	13.2
12–18	94.4	111.1	118.1	104.4	97.2	80.5	89.2	51.1	44.8	45.7	29.3	41.9	19.3	33.1	14.4	35.6	13.2
18–24	121.2	129.7	173.4	94.4	79.1	57.2	55.2	54.0	46.9	50.4	66.2	76.4	51.5	73.7	67.6	57.7	99.9
24–30	31.1	25.5	40.3	23.6	32.9	16.3	24.0	19.1	13.8	10.5	9.9	10.4	8.3	11.3	7.8	8.5	8.4
30–36	9.0	2.9	1.3	0.4	0.1	0	0	0.1	0	0.1	0	0	0	0	0	0.2	0.1
36–42	103.6	97.9	112.9	79.0	67.4	65.3	57.1	43.2	61.9	57.5	69.9	76.1	67.6	66.2	82.6	52.6	50.4
42–48	27.1	16.1	7.4	11.0	4.8	1.0	2.4	1.3	0.9	0.3	0.4	0.3	0.3	0.4	0.1	0.8	0.1
48–54	0.1	0.1	0.1	0.1	0.1	0	0.1	0	0	0	0	0	0	0	0	0	0

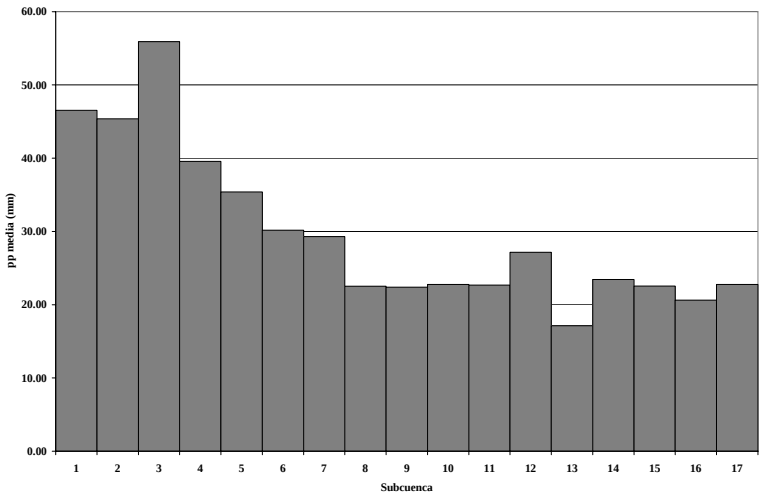

Fig. 8 Distribution of total rainfall over the sub-basins. Procedure 1.

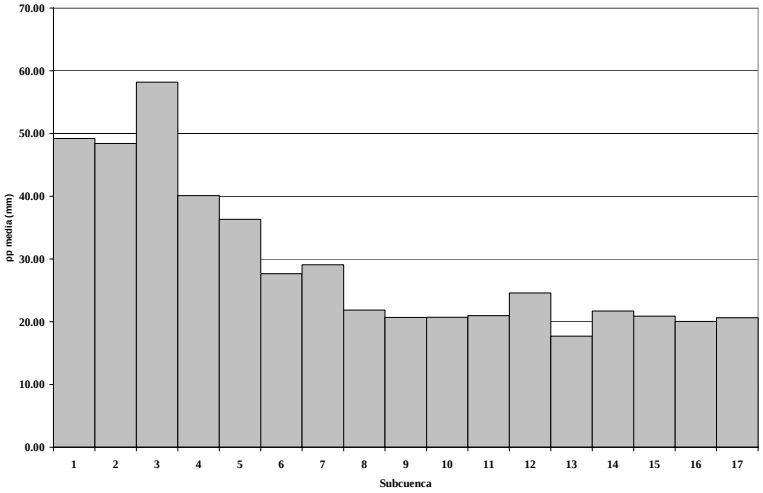

Fig. 9 Distribution of total rainfall over the sub-basins. Procedure 2.

Figures 8 and 9 show the distribution of total rainfall over each one of the 17 sub-basins obtained by the two abovementioned procedures.

CONCLUSIONS

This work evidences the usefulness of remote sensing methods in the estimation of rainfall fields.

When changing from 6-h to 3-h consecutive lapses, the comparison between area-averaged rainfall values obtained by means of procedures 1 and 2 (with and without time-interpolated synthetic temperature images) showed a significant increase in the differences in time distribution of rainfall depths. These results evidence the importance of having detailed rainfall fields integrated over short lapses.

The results show that the generation of synthetic temperature images before the use of the "autoestimator" technique allows the capture of the displacement of rain cloud cells, which at the same time causes significant differences in estimated rainfall over areas smaller than the size of the studied watershed.

Differences between areal rainfall estimates generated by means of procedures 1 and 2 are evidence of the importance of making a correct description of the displacement of rain cloud cells to get better estimations of precipitation fields by remote sensing methods.

Acknowledgements This work was partially supported by Grant no. 07-9743 of Agencia Nacional de Promoción Científica y Tecnológica. GOES-8 images and gridded meteorological fields were provided by Servicio Meteorológico Nacional.

REFERENCES

Barrera, D., Marcuzzi, E. & Naumann, G. (2001) Desarrollo del software de un Sistema Operativo de estimación de precipitación a partir de imágenes GOES. In: *IX Congreso Latinoamericano e Ibérico de Meteorología* (Buenos Aires, Argentina, 5–9 May 2001).

Barrera, D. (2007) The generation of synthetic brightness temperature images to improve rainfall estimation from GOES satellite. In: *Predictions in Ungauged Basins: PUB Kick-off* (Proc. PUB Kick-off meeting held in Brasilia, 20–22 November 2002). IAHS Publ. 309. IAHS Press, Wallingford, UK (this issue).

Barrera, D., Ceirano, E. & Zucarelli, G. (2002) Determinación de precipitación por subcuencas en el Arroyo Feliciano a partir de imágenes del satélite GOES-8. In: *XIX Congreso Nacional del Agua* (Villa Carlos Paz, Argentina, 12–16 August).

Horton, R. E. (1923) Accuracy of areal rainfall estimates. *Mon Weather Rev*. **51**, 348–353.

Lebel, T., Bastin, G., Obled, C. & Creutin, J. D. (1987) On the accuracy of areal rainfall estimation: A case study. *Water Resour. Res.* **23**(11), 2123–2134.

Vicente, G., Scofield, R. & Menzel, P. (1998) The operational GOES infrarred rainfall estimation technique. *Bull. Am. Meteorol*. **79**, 1883–1898.